(He^3,pp) Reaction*

E. M. HENLEY AND C. E. LACY
Department of Physics, University of Washington, Seattle, Washington
(Received 13 February 1967)

The (He^3,pp) stripping reaction is studied in the distorted-wave Born approximation, with simplifying assumptions which allow a two-body formulation of the problem. Two limiting cases are investigated. (1) The emerging protons are closely correlated; their final-state interaction with each other is treated appropriately, but those with the nucleus are approximated by one with the center of mass of the pair. (2) The protons interact individually with the residual nucleus but their mutual interaction is neglected. It is found that for a given relative momentum **q** of the two protons the angular distribution for the recoiling residual nucleus is essentially the same for the two cases. However, the differential cross section depends only on the magnitude of **q** in case (1), whereas it depends on both the magnitude *and* direction of **q** for case (2). Thus, an experimental distinction between the limiting cases should be possible.

I. INTRODUCTION

STRIPPING reactions have been widely employed in the study of nuclear spectroscopy. Most of the reactions studied so far have a single emergent particle in the final state, so that there is no degree of freedom in the kinematics, given the scattering angle and the state of the residual nucleus.

In this work we investigate the (He^3,pp) reaction, which is the simplest stripping reaction with multiple (unbound) emergent particles in the final state. From such reactions one could hope to learn more about the mode of nuclear excitation in the stripping process, by a measurement of the correlation between the two emergent protons. The (He^3,pp) reaction is also of interest because it allows excitation of isospin states in the residual nucleus which cannot be reached by an analogous reaction in which only one particle emerges, such as (d,p) stripping. In the latter case, if a deuteron is incident on a target of isospin zero, and if isospin is conserved, then the residual nucleus must be in a state with isospin equal to $\frac{1}{2}$. For a (He^3,pp) reaction with the same target, the residual nucleus may have isospin equal to $\frac{3}{2}$ or $\frac{1}{2}$. The simple stripping model, with no core excitation, predicts that only isospin-$\frac{1}{2}$ states are populated. This assertion is clearly amenable to experimental investigation.

In this paper we do not consider core excitation. With this simplification we treat (He^3,pp) stripping for two limiting cases: (1) The emerging protons are closely correlated and their final-state interaction with each other is treated appropriately, but those with the nucleus are approximated by one with the pp center of mass, and (2) the protons interact individually with the residual nucleus but their mutual interaction is neglected. There has been some discussion whether final-state effects are measurable[1]; our results suggest that a (He^3,pp) experiment can be used to detect such final-state rescattering.

In Sec. II we formulate the problem, for the two limiting cases mentioned above, in the distorted-wave Born approximation using optical potentials in the incoming and outgoing channels determined from elastic scattering (Sec. III). The results of the calculations are presented in Sec. IV and discussed in Sec. V.

In the present paper we restrict ourselves to a two-body formulation; this necessarily involves some approximations (Sec. II). A more exact analysis of the (He^3,pp) reaction would involve a correct treatment of a four-body problem, viz., the target nucleus (taken as one particle), the captured neutron, and the two emergent protons. This can be done, at least in principle, by an extension of the Faddeev formalism.[2] This aspect of the problem is currently being investigated.

II. THEORETICAL DEVELOPMENT

A. Introduction

The theory of direct nuclear reactions in a distorted-wave Born-approximation (DWBA) framework has been treated extensively in the literature[3] so that only the matrix is given here,

$$\mathfrak{M} \approx \langle X_f^- | V_{n1} + V_{n2} | X_i^+ \rangle . \quad (1)$$

We assume the following: (a) The initial nucleus, or "core," acts merely as a spectator and is unaffected by the reaction. (b) The residual nucleus is left in a single-particle state of well-defined total and orbital angular momenta; for simplicity, we assume that this corresponds to the ground state. (c) The j-j coupling scheme is applicable. (d) The captured nucleon is bound in a finite Saxon well. (e) The interaction potentials responsible for the reaction [V_{n1} and V_{n2} in Eq. (1)] are spin-isospin-independent central potentials. Although these assumptions are not essential, they are physically reasonable and simplify the calculation considerably.

For a target of A nucleons, the center-of-mass system

* Supported in part by the U. S. Atomic Energy Commission under Contract No. RLO-1388B.
[1] Č. Zupančič, Rev. Mod. Phys. 37, 330 (1965).
[2] V. A. Alessandrini, J. Math. Phys. 7, 215 (1966).
[3] See, e.g., W. Tobocman, *Theory of Direct Nuclear Reactions* (Oxford University Press, New York, 1961).

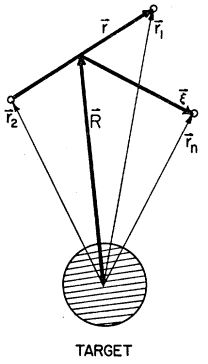

FIG. 1. Pictorial representation of the relation between the vectors $\mathbf{r}_1$, $\mathbf{r}_2$, $\mathbf{r}_n$, $\mathbf{R}$, $\mathbf{r}$, and $\boldsymbol{\xi}$. The heavy arrows indicate the coordinates used in the $\mathbf{R}$, $\mathbf{r}$ formulation [Sec. IIB]; the light arrows indicate the coordinates used in the $\mathbf{r}_1$, $\mathbf{r}_2$ formulation [Sec. IIC].

optical-model wave functions for the initial and final states are (the notation of Henley and Yu is used,[4] with $\hbar=c=1$)

$$X_i^+=\chi_{\mathbf{K}}^+(\mathbf{R}+\tfrac{1}{3}\boldsymbol{\xi})\Phi_i(1,\cdots,A)\phi_{\mathrm{He}}(\boldsymbol{\xi},\mathbf{r}) \times[\zeta_{1/2}{}^{\mu}(\mathrm{He})\rho_{1/2}{}^{1/2}(\mathrm{He})], \quad (2)$$

$$X_f^-=\chi_{\mathbf{k}',\mathbf{k}''}^-(\mathbf{r}_1,\mathbf{r}_2)\Phi_f(1,\cdots,A+1)\zeta(1,2)\rho(1,2), \quad (3)$$

where $\mathbf{R}$, $\mathbf{r}_1$, $\mathbf{r}_2$, and $\mathbf{r}_n$ are measured relative to the initial nuclear center; $\mathbf{R}$ is the position of the pp center of mass, $\mathbf{r}_1$ is that of proton 1, $\mathbf{r}_2$ that of proton 2, and $\mathbf{r}_n$ that of the neutron. We have introduced the vectors $\mathbf{r}\equiv\mathbf{r}_1-\mathbf{r}_2$ and $\boldsymbol{\xi}\equiv\mathbf{r}_n-\mathbf{R}$. The relations between $\mathbf{r}_1$, $\mathbf{r}_2$, $\mathbf{r}_n$, $\mathbf{R}$, $\mathbf{r}$ and $\boldsymbol{\xi}$ are shown in Fig. 1. The subscript $\mathbf{K}$ is the momentum of the incident He^3 particle, and the pair of momenta $\mathbf{k}'$, $\mathbf{k}''$ refer to the final pp system; their choice depends on the formulation of the problem [see Secs. IIB and IIC].

In Eqs. (2) and (3), χ^+ and χ^- are the distorted waves representing the incoming and outgoing particles, respectively, with the $+(-)$ sign denoting outgoing (incoming) boundary conditions. Φ_i is a completely antisymmetric space-spin-isospin internal nuclear wave function of total angular momentum J_i and isospin t_i, having third components M_i and ν_i; Φ_f is defined analogously for the final nucleus. $\phi_{\mathrm{He}}(\boldsymbol{\xi},\mathbf{r})$ is the space part of the He^3 internal wave function. ζ is a spin state and ρ an isospin-state function, with the square bracket in Eq. (2) denoting the completely antisymmetric spin-isospin state function for He^3.[4]

We expand the wave function for the $(A+1)$ particles of the residual nucleus in terms of the wave function for the A particles of the initial nucleus and the possible neutron states:

$$\Phi_f(1,\cdots,A+1)=\sum_{J_i',M_i',t_i',\nu_i'} B(t_i',t_f;J,J_i',J_f) \times(t_i'\tfrac{1}{2}\nu_i'-\tfrac{1}{2}|t_f\nu_f)(J_i'JM_i'M|J_fM_f) \times\Phi_{i'}(1,\cdots,A)\phi_J{}^M(\mathbf{r}_n). \quad (4)$$

In Eq. (4) the expansion coefficients $B(t_i',t_f;J,J_i,'J_f)$ are related[4] to the usual spectroscopic factors; the symbols $(j_1j_2m_1m_2|jm)$ are Clebsch-Gordan coefficients, and the subscript i' on Φ indicates quantum numbers J_i', M_i', t_i', and ν_i'. The $\phi_J{}^M$ is the bound-state wave function for the captured particle, and can be written as

$$\phi_J{}^M(\mathbf{r}_n)=\sum_{m,s}(l\tfrac{1}{2}ms|JM)\Re_l(r_n) \times Y_l{}^m(\hat{r}_n)\zeta_{1/2}{}^s(n)\rho_{1/2}{}^{-1/2}(n), \quad (5)$$

where $\Re_l(r_n)$ is the radial part of the wave function for the captured nucleon in a finite Saxon well, and $Y_l{}^m(\hat{r}_n)$ is a spherical harmonic of the angle defined by the unit vector $\hat{r}_n$.

At this point we introduce some specific assumptions regarding the form of the pp wave function $\chi_{\mathbf{k}',\mathbf{k}''}^-(\mathbf{r}_1,\mathbf{r}_2)$. We consider two limiting cases, viz.: (1) The protons come off close together as an unbound "diproton" with low relative energy ϵ_f, so that for the small distances relevant in this problem we may take the relative orbital angular momentum and total spin of the pp wave function to be zero. In this case it is convenient to use the coordinates $\mathbf{R}$ and $\mathbf{r}$. We refer to this as the "$\mathbf{R}$, $\mathbf{r}$ formulation". (2) The protons come off with considerable relative energy ϵ_f, i.e., in quite divergent directions, so that their final-state interaction with each other is negligible, $v(\mathbf{r})\approx 0$. We refer to this as the "$\mathbf{r}_1$, $\mathbf{r}_2$ formulation". Although these are but two possible options, they describe limiting situations, which we believe to apply in the present problem.

B. R, r Formulation

In this formulation we approximate the interaction of the nucleus with the individual protons in the final state by one with the center of mass of the pp pair as though it were a single particle.[4,5] The Hamiltonian for the pp pair then separates:

$$H(1,2)=-\nabla_{\mathbf{R}'}{}^2/2M+V(\mathbf{R}')-\nabla_{\mathbf{r}}{}^2/2\mu+v(\mathbf{r}) =H(\mathbf{R}')+h(\mathbf{r}). \quad (6)$$

In Eq. (6), the masses M and μ are $M=m_1+m_2$, $\mu=m_1m_2/(m_1+m_2)$, and the vector $\mathbf{R}'$ is the position of the center of mass of the pp pair relative to the residual nucleus. With the above assumption the pp distorted wave function is a product,

$$\chi_{\mathbf{k}',\mathbf{k}''}^-(\mathbf{r}_1,\mathbf{r}_2)=\chi_{\mathbf{k},\mathbf{q}}^-(\mathbf{R}',\mathbf{r}) =\chi_{\mathbf{k}}^-\left(\frac{A}{A+1}\mathbf{R}-\frac{1}{A+1}\boldsymbol{\xi}\right) \times\chi_{\mathbf{q}}^-(\mathbf{r})\zeta_0{}^0(1,2)\rho_1{}^1(1,2), \quad (7)$$

where $\mathbf{k}$ is the total momentum operator of the pp pair

[4] E. M. Henley and D. U. L. Yu, Phys. Rev. 133, 1445 (1964).

[5] E. M. Henley, in *Preludes in Theoretical Physics in Honor of V. F. Weisskopf*, edited by A. de-Shalit, H. Feshbach, and L. van Hove (North-Holland Publishing Company, Amsterdam, 1966), p. 89.

and $\mathbf{q}$ is that for their relative momentum,

$$\mathbf{q}=(\mathbf{k}_1-\mathbf{k}_2)/2.$$

Inserting Eqs. (4), (5), and (7) into Eq. (3) we have for X_f^-:

$$X_f^-=\sum_{J_i',M_i',t_i',\nu_i',m,s} B(t_i',t_f;\,J,J_i',J_f)\times(t_i'\tfrac{1}{2}\nu_i'-\tfrac{1}{2}|t_f\nu_f)(J_i'JM_i'M|J_fM_f)\times(l\tfrac{1}{2}ms|JM)\chi_k^-\left(\frac{A}{A+1}\mathbf{R}-\frac{1}{A+1}\xi\right)\chi_q^-(\mathbf{r})\times\Phi_i(1,\cdots,A)\mathfrak{R}_l(r_n)Y_l^m(\hat{r}_n)\times\zeta_{1/2}^m(n)\rho_{1/2}^{-1/2}(n)\zeta_0^0(1,2)\rho_1^1(1,2). \quad (8)$$

In terms of the matrix element $\mathfrak{M}$, the differential cross section is given by

$$\frac{d^2\sigma}{d\epsilon_f d\Omega_k}=2\pi\frac{\mu_i}{K}\frac{d^2\rho}{d\epsilon_f d\Omega_k}\overline{\sum}|\mathfrak{M}|^2, \quad (9)$$

where μ_i is the reduced mass of the He^3 particle and the initial nucleus, Ω_k denotes the solid angle for $\mathbf{k}$, and $d^2\rho/d\epsilon_f d\Omega_k$ is the density of available final states. The bar over the summation sign symbolizes the usual average and sum over initial- and final-state magnetic quantum numbers, respectively. After integrating over the coordinates of the A nucleons, averaging over M_i, summing over M_f, and doing the spin-isospin sums we find (for the fixed orbital angular momentum l of the captured nucleon)

$$\frac{d^2\sigma}{d\epsilon_f d\Omega_k}=2\pi\frac{\mu_i}{K}\frac{d^2\rho}{d\epsilon_f d\Omega_k}\frac{1}{6}\frac{1}{2l+1}\frac{2J_f+1}{2J_i+1}B^2(t_i,t_f;\,J,J_i,J_f)\times(t_i\tfrac{1}{2}\nu_i-\tfrac{1}{2}|t_f\nu_f)^2\sum_m|\mathfrak{M}_l^m|^2, \quad (10)$$

where

$$\mathfrak{M}_l^m=\left\langle\chi_k^-\left(\frac{A}{A+1}\mathbf{R}-\frac{1}{A+1}\xi\right)\chi_q^-(\mathbf{r})\mathfrak{R}_l(r_n)Y_l^m(\hat{r}_n)|\times(V_{n1}+V_{n2})|\chi_K^+(\mathbf{R}+\tfrac{1}{3}\xi)\phi_{He}(\xi,\mathbf{r})\right\rangle. \quad (11)$$

For simplicity we assume a symmetric Gaussian for the He^3 internal wave function,[4]

$$\phi_{He}(\xi,\mathbf{r})=N_{He}\times\exp\{-\tfrac{1}{2}\gamma^2[(\mathbf{r}_1-\mathbf{r}_2)^2+(\mathbf{r}_2-\mathbf{r}_n)^2+(\mathbf{r}_n-\mathbf{r}_1)^2]\}=N_{He}\exp\{-\tfrac{1}{2}\gamma^2(\tfrac{3}{2}r^2+2\xi^2)\}, \quad (12)$$

where N_{He} is a normalization constant,

$$N_{He}=\gamma^3 3^{3/4}\pi^{-3/2},$$

and[4] $\gamma\approx0.36$ F^{-1} as determined from electron scattering.

The interaction potential is also taken to be a Gaussian,

$$V_{n1}+V_{n2}=V_0[\exp\{-\beta^2(\mathbf{r}_n-\mathbf{r}_1)^2\}+\exp\{-\beta^2(\mathbf{r}_n-\mathbf{r}_2)^2\}]=V_0[\exp\{-\beta^2(\xi-\tfrac{1}{2}\mathbf{r})^2\}+\exp\{-\beta^2(\xi+\tfrac{1}{2}\mathbf{r})^2\}], \quad (13)$$

with[4] $V_0\approx70$ MeV and $\beta^2\approx0.4$ F^{-2}, to obtain an approximate match to the nucleon-nucleon low-energy elastic scattering.

For purposes of computing the overlap of the neutron wave functions in the matrix element, we neglect ξ relative to $\mathbf{R}$. We justify this roughly by considering the behavior of the He^3 internal wave function and the interaction potential; both of these are exponentially decreasing functions of ξ^2. Since the optical potentials used in calculating χ_K^+ and χ_k^- give rise to strong absorption, the main contribution to the overlap integrals in $\mathfrak{M}_l^m$ comes from a region close to the nuclear surface, $R\approx R_{Nuclear}\approx1.25A^{1/3}$. For sufficiently large A, therefore, the above-mentioned exponential factors will be small for ξ comparable in magnitude to the nuclear radius. We therefore approximate as follows:

$$\frac{A}{A+1}\mathbf{R}-\frac{1}{A+1}\xi\approx\frac{A}{A+1}\mathbf{R}, \quad (14a)$$

$$\mathbf{r}_n=\mathbf{R}+\xi\approx\mathbf{R}, \quad (14b)$$

$$\mathbf{R}+\tfrac{1}{3}\xi\approx\mathbf{R}. \quad (14c)$$

Thus, we find for $\mathfrak{M}_l^m$:

$$\mathfrak{M}_l^m=\left\langle\chi_k^-\left(\frac{A}{A+1}\mathbf{R}\right)\chi_q^-(\mathbf{r})\mathfrak{R}_l(R)Y_l^m(\hat{R})|\times(V_{n1}+V_{n2})|\chi_K^+(\mathbf{R})\phi_{He}(\xi,\mathbf{r})\right\rangle. \quad (15)$$

We expand the incoming and outgoing wave functions in partial waves, taking the initial momentum $\mathbf{K}$ as the axis of quantization:

$$\chi_K^+(\mathbf{R})=\sum_{L'}\frac{1}{KR}i^{L'}[4\pi(2L'+1)]^{1/2}\times U_{KL'}^+(R)Y_{L'}^0(\hat{R}), \quad (16)$$

$$\chi_k^-\left(\frac{A}{A+1}\mathbf{R}\right)=\sum_{L,N}\frac{A+1}{A}\frac{4\pi}{kR}i^L U_{kL}^-\left(\frac{A}{A+1}R\right)\times Y_L^N(\hat{R})Y_L^{N*}(\hat{k}). \quad (17)$$

Inserting Eqs. (16) and (17) into Eq. (11) we can do the integration over the internal variable ξ and the angular integrations for $\mathbf{R}$ and $\mathbf{r}$. $\mathfrak{M}_l^m$ thus reduces to

$$\mathfrak{M}_l^m=\frac{4\pi}{kK}\frac{A+1}{A}\sum_{L,L'}((2L+1)(2l+1))^{1/2}\times(Ll-mm|L'0)(Ll00|L'0)Y_L^{-m}(\hat{k})i^{L'-L}Dd, \quad (18)$$

where d and D are

$$d=\frac{8\pi\gamma^3 3^{3/4}V_0}{(\beta^2+\gamma^2)^{3/2}}\int_0^\infty \chi_q^-(\mathbf{r}) \times\exp\left\{-\frac{\beta^2\gamma^2+0.75\gamma^4}{\beta^2+\gamma^2}r^2\right\}r^2dr, \quad (19)$$

$$D=\int_0^\infty U_{kL}^+\left(\frac{A}{A+1}R\right)U_{KL'}^+(R)\Re_l(R)dR. \quad (20)$$

We have used the relation

$$U_{kL}^{-*}\left(\frac{A}{A+1}R\right)=U_{kL}^+\left(\frac{A}{A+1}R\right)$$

to obtain D in the form given by Eq. (20).

The integration over R is part of a numerical program which computes a quantity $\sigma(\Theta)$ given by

$$\sigma(\Theta)=\frac{16\pi^2}{k^2K^2}(2l+1)\sum_m|\sum_{L,L'}(2L+1)^{1/2}(Ll-mm|L'0) \times(Ll00|L'0)Y_L^{-m}(\Theta,0)D|^2. \quad (21)$$

The partial-wave amplitudes U^+ are obtained from MSCAT-4 (a modified form of the UCLA SCAT-4 code[6]) which gives normalized wave functions as output. Inserting the density-of-states factor we have finally

$$\frac{d^2\sigma}{d\epsilon_f d\Omega_k}=\frac{\mu_i\mu_f}{16\pi^4}\frac{k}{K}(m_N{}^3\epsilon_f)^{1/2}\left(\frac{A+1}{A}\right)^2\frac{1}{6}\frac{1}{2l+1}\frac{2J_f+1}{2J_i+1} \times B^2(t_i,t_f;J,J_i,J_f)(t_i\tfrac{1}{2}\nu_i-\tfrac{1}{2}|t_f\nu_f)^2|d|^2\sigma(\Theta), \quad (22)$$

where m_N is the nucleon mass and μ_f is the reduced mass of the pp system and the residual nucleus.

C. $\mathbf{r}_1$, $\mathbf{r}_2$ Formulation

In this formulation we assume that the protons interact individually with the nucleus, and we effectively neglect their interaction with each other. The Hamiltonian is then given by

$$H(1,2)=-\nabla_1{}^2/2m_1+V(\mathbf{r}_1)-\nabla_2{}^2/2m_2+V(\mathbf{r}_2) =H(1)+H(2), \quad (23)$$

where $V(\mathbf{r}_1)$ includes only the interaction of proton 1 with the residual nucleus, and similarly for $V(\mathbf{r}_2)$. Although, in the spirit of Sec. IIA, we could consider the interactions $V(\mathbf{r}_1)$ and $V(\mathbf{r}_2)$ to include an average interaction of the two protons with each other, we do not do this here; rather we assume that $V(\mathbf{r}_1)$ and $V(\mathbf{r}_2)$ are determined by elastic proton scattering. With Eq. (23) the final-state wave function becomes

$$X_f^-=\chi_1^-(\mathbf{r}_1)\chi_2^-(\mathbf{r}_2)\zeta(1,2)\rho(1,2)\Phi_f(1,\cdots,A+1), \quad (24)$$

where the subscripts 1 and 2 denote momenta $\mathbf{k}_1$ and $\mathbf{k}_2$, respectively. We take the undetermined variables in the differential cross section to be E_1, Ω_1, and Ω_2, where E_1 is the kinetic energy of proton 1, Ω_1 is the associated solid angle, and Ω_2 is the corresponding solid angle for proton 2. These variables are most accessible experimentally; any other choice can be obtained by a suitable transformation. Substituting Eq. (24) into Eq. (9), we integrate over the A nuclear coordinates, do the implied average and sum over M_i and M_f, respectively, and carry out the spin-isospin sums to obtain

$$\frac{d^3\sigma}{dE_1d\Omega_1d\Omega_2}=2\pi\frac{\mu_i}{K}\frac{d^3\rho}{dE_1d\Omega_1d\Omega_2}\frac{1}{6}\frac{1}{2l+1}\frac{2J_f+1}{2J_i+1} \times B^2(t_i,t_f;J,J_i,J_f)(t_i\tfrac{1}{2}\nu_i-\tfrac{1}{2}|t_f\nu_f)^2\sum_m|M_l{}^m|^2, \quad (25)$$

where now

$$M_l{}^m=\langle\chi_1^-(\mathbf{r}_1')\chi_2^-(\mathbf{r}_2')\Re_l(r_n)Y_l{}^m(\hat{r}_n)| \times V_{n1}+V_{n2}|\chi_K^+(\Re)\phi_{\mathrm{He}}\rangle, \quad (26)$$

$\Re=\frac{1}{3}(\mathbf{r}_1+\mathbf{r}_2+\mathbf{r}_n)$, and the primes on $\mathbf{r}_1'$ and $\mathbf{r}_2'$ mean that they are relative to the center of mass of the residual nucleus, rather than the initial nucleus.

In order to make the nine-dimensional integral of Eq. (26) tractable we introduce a simplification which has been widely employed in deuteron stripping calculations, viz., we assume that capture takes place at a point, with

$$\lim_{\beta\to\infty}V_0e^{-\beta^2r^2}\longrightarrow\pi^{3/2}V_0\beta^{-3}\delta^3(\mathbf{r}), \quad (27)$$

where

$$V_0\beta^{-3}=\text{constant}=70\text{ MeV}\times(0.4)^{-3/2}\text{ F}^3 =277\text{ MeV F}^3. \quad (28)$$

Introducing the coordinates

$$\boldsymbol{\varrho}=\tfrac{2}{3}\mathbf{r}_1+\tfrac{1}{3}\mathbf{r}_2, \quad (29a)$$

$$\mathbf{r}=\mathbf{r}_1-\mathbf{r}_2, \quad (29b)$$

and inserting the delta-function interaction potentials we have for the matrix $M_l{}^m$:

$$M_l{}^m=2\pi^{3/2}\beta^{-3}N_{\mathrm{He}}V_0\int\chi_1^{-*}\left(\frac{A}{A+1}[\boldsymbol{\varrho}+\tfrac{1}{3}\mathbf{r}]\right) \times\chi_2^{-*}\left(\frac{A}{A+1}\left[\boldsymbol{\varrho}-\left(\frac{2}{3}+\frac{1}{A}\right)\mathbf{r}\right]\right) \times\chi_K^+(\boldsymbol{\varrho})\psi^*(\boldsymbol{\varrho}+\tfrac{1}{3}\mathbf{r})e^{-\gamma^2r^2}d^3\rho d^3r, \quad (30)$$

where

$$\psi^*(\boldsymbol{\varrho}+\tfrac{1}{3}\mathbf{r})=\Re_l(|\boldsymbol{\varrho}+\tfrac{1}{3}\mathbf{r}|)Y_l{}^{m*}\left(\frac{\boldsymbol{\varrho}+\frac{1}{3}\mathbf{r}}{|\boldsymbol{\varrho}+\frac{1}{3}\mathbf{r}|}\right).$$

[6] M. A. Melkanoff, J. S. Nodvik, D. S. Saxon, and D. G. Cantor, *A Fortran Program for Elastic Scattering Analyses with the Nuclear Optical Model* (University of California Press, Berkeley, California, 1961).

The r integration can be performed in the following way[7,8]: Define $e^{-\gamma^2 r^2} \equiv f(r^2)$. Introduce the Fourier transform

$$f(\lambda^2) = \int e^{i\lambda\cdot r} f(r^2) d^3r, \tag{31}$$

and its inverse

$$f(r^2) = (2\pi)^{-3} \int e^{-i\lambda\cdot r} \tilde{f}(\lambda^2) d^3\lambda. \tag{32}$$

If we expand $\tilde{f}(\lambda^2)$ in a Taylor series about $\lambda^2 = 0$ we obtain for $f(r^2)$,

$$f(r^2) \rightarrow \sum_{n=0}^{\infty} \pi^{3/2}\gamma^{-3} \frac{1}{n!}\left(\frac{\nabla_r^2}{4\gamma^2}\right)^n \delta^3(\mathbf{r}). \tag{33}$$

Recalling the property of delta functions,

$$\int_{-\infty}^{\infty} \delta^m(x) f(x) dx = (-)^m f^m(0), \tag{34}$$

and substituting Eq. (33) in Eq. (30), we find for M_l^m:

$$M_l^m = 2\pi^3\beta^{-3}\gamma^{-3} N_{\mathrm{He}} V_0 \int \chi_K^+(\varrho) \left\{ \sum_{n=0}^{\infty} \frac{1}{n!}\left(\frac{\nabla_r^2}{4\gamma^2}\right)^n \right.$$

$$\times \left[\chi_1^{-*}\left(\frac{A}{A+1}[\varrho + (1/3)\mathbf{r}]\right) \chi_2^{-*}\left(\frac{A}{A+1}\left[\varrho - \left((2/3)+\frac{1}{A}\right)\mathbf{r}\right]\right) \psi^*(\varrho + (1/3)\mathbf{r}) \right] \Bigg\}_{r=0} d^3\rho = 2\pi^3\beta^{-3}\gamma^{-3} N_{\mathrm{He}} V_0 \int \chi_K^+(\varrho)$$

$$\times \left\{ \exp\left[\frac{1}{4\gamma^2}((1/9)\nabla_1^2 + (9/16)\nabla_2^2 + (1/9)\nabla_n^2 - (1/2)\nabla_1\cdot\nabla_2 + (2/9)\nabla_1\cdot\nabla_n - (1/2)\nabla_2\cdot\nabla_n)\right] \right.$$

$$\left. \times \left[\chi_1^{-*}\left(\frac{A}{A+1}\varrho\right) \chi_2^{-*}\left(\frac{A}{A+1}\varrho\right) \psi^*(\varrho) \right] \right\} d^3\rho, \tag{35}$$

where ∇_1 operates only on $\chi_1^{-*}[A\varrho/(A+1)]$, ∇_2 only on $\chi_2^{-*}[A\varrho/(A+1)]$, and ∇_n only on $\psi^*(\varrho)$. We can write

$$(1/9)(\nabla_1^2 + (81/16)\nabla_2^2 + \nabla_n^2 - (9/2)\nabla_1\cdot\nabla_2 + 2\nabla_1\cdot\nabla_n - (9/2)\nabla_2\cdot\nabla_n)$$
$$= (1/36)(4\nabla_1^2 + (81/4)\nabla_2^2 + 4\nabla_n^2 - 18\nabla_1\cdot\nabla_2 + 8\nabla_1\cdot\nabla_n - 18\nabla_2\cdot\nabla_n)$$
$$= (1/36)(13\nabla_1^2 + (117/4)\nabla_2^2 + 13\nabla_n^2 + 26\nabla_1\cdot\nabla_n - 9\nabla^2), \tag{36}$$

where $\nabla = \nabla_1 + \nabla_2 + \nabla_n$ operates on the product

$$\chi_1^{-*}\left(\frac{A}{A+1}\varrho\right) \chi_2^{-*}\left(\frac{A}{A+1}\varrho\right) \psi^*(\varrho).$$

We have investigated the magnitude of the contribution from the 26 $\nabla_1\cdot\nabla_n$ terms for the case of plane waves, i.e., $e^{i\mathbf{k}_1\cdot\rho} e^{i\mathbf{k}_2\cdot\rho} \psi^*(\varrho)$, and, at the energies utilized in this work, found it to be small compared to the contributions from the other terms in Eq. (36). We assume that this will be true for the DWBA case also. Then, by repeated application of Green's theorem Eq. (35) becomes

$$M_l^m = 2\pi^3\beta^{-3}\gamma^{-3} N_{\mathrm{He}} V_0 \int \left[e^{-(9\nabla^2/144\gamma^2)} \chi_K^+(\varrho)\right] \left[e^{(13\nabla_1^2/144\gamma^2)} \chi_1^{-*}\left(\frac{A}{A+1}\varrho\right)\right]$$

$$\times \left[e^{(117\nabla_2^2/576\gamma^2)} \chi_2^{-*}\left(\frac{A}{A+1}\varrho\right)\right] \left[e^{(13\nabla_n^2/144\gamma^2)} \psi^*(\varrho)\right] d^3\rho. \tag{37}$$

If we also assume that the gradients of the potentials are negligible in comparison with the gradients of the wave functions, so that we can write $(\nabla^2)^n \approx [2m(V-E)]^n$, then Eq. (37) becomes[9]

$$M_l^m = 2\pi^3\beta^{-3}\gamma^{-3} N_{\mathrm{He}} V_0 \exp\left[\frac{9K^2 - (144/169)\times 13k_1^2 - (144/169)\times(117/4)k_2^2 + 13\alpha^2}{144\gamma^2}\right]$$

$$\times \int g(\rho) \chi_1^{-*}\left(\frac{A}{A+1}\varrho\right) \chi_2^{-*}\left(\frac{A}{A+1}\varrho\right) \psi^*(\varrho) \chi_K^+(\varrho) d^3\rho, \tag{38}$$

[7] Gy. Bencze and J. Zimanyi, Phys. Letters **9**, 246 (1964).
[8] F. G. Perey and D. S. Saxon, Phys. Letters **10**, 107 (1964).
[9] Gy. Bencze and J. Zimanyi, Nucl. Phys. **81**, 76 (1966).

where $\alpha^2/2m$ is the binding energy of the captured nucleon, and

$$g(\rho)=\exp\left[\frac{-18m_{\mathrm{He}}V_{\mathrm{He}}+(144/169)\times 26m_1V_1+(144/169)\times(117/2)m_2V_2+26m_nV_n}{144\gamma^2}\right]. \tag{39}$$

Expanding the distorted waves in partial waves as before we find

$$\frac{d^3\sigma}{dE_1d\Omega_1d\Omega_2}=8\pi\frac{\mu_i}{K}\frac{d^3\rho}{dE_1d\Omega_1d\Omega_2}\frac{1}{6}\frac{1}{2l+1}\frac{2J_f+1}{2J_i+1}B^2(t_i,t_f;J,J_iJ_f)$$

$$\times(t_i\tfrac{1}{2}\nu_i-\tfrac{1}{2}|t_f\nu_f)^2\pi^6\beta^{-6}\gamma^{-6}N_{\mathrm{He}}{}^2V_0{}^2\sum_m\left|\sum_{L,\lambda,l_1,l_2,m_1}\left(\frac{A+1}{A}\right)^2(4\pi)^{3/2}\right.$$

$$\times((2l_1+1)(2l_2+1)(2l+1))^{1/2}i^{L-l_1-l_2}(l_1l_2-m_1m_1+m|\lambda m)(l^1l_200|\lambda 0)$$

$$\times(l\lambda-mm|L0)(l\lambda00|L0)(1/Kk_1k_2)Y_{l_1}{}^{-m_1}(\hat{k}_1)Y_{l_2}{}^{m_1+m}(\hat{k}_2)$$

$$\left.\times\int U_{KL}{}^+(\rho)U_{k_1l_1}{}^+\left(\frac{A}{A+1}\rho\right)U_{k_2l_2}{}^+\left(\frac{A}{A+1}\rho\right)\Re_l(\rho)g(\rho)\rho^{-1}d\rho\right|^2. \tag{40}$$

Equation (40) is evaluated numerically by a program which computes the quantity $\sigma(\Theta_1,\Theta_2)$ given by

$$\sigma(\Theta_1,\Theta_2)=\sum_m\Big|\sum_{L,\lambda,l_1,l_2,m_1}\cdots\Big|^2. \tag{41}$$

III. DETERMINATION OF OPTICAL PARAMETERS

If the incident energy of the He^3 projectiles is sufficiently high and the final-state pp relative energy ϵ_f is sufficiently small, then it is possible to relate the $A(He^3,pp)A'$ differential cross section directly to that *measured* for the $A(He^3,d)A''$ reaction.[5,10] This relation requires (1) that the **R**, **r** formulation is valid; (2) that the binding energy of the deuteron ϵ_d and ϵ_f are both much smaller than the incident energy (the ϵ_f dependence of the cross section is *not* neglected); (3) that the difference between the Coulomb interaction of the two protons with the final nucleus A' and that of the deuteron with A'' can be neglected; (4) that the nuclear optical potential of the pp center of mass with A' is identical to that of the deuteron with the nucleus A''. This last requirement assumes that the spin and isospin dependences of the optical potentials are small. For instance, spin-orbit effects must be neglected, since the spin of the deuteron and that of the pp system are different; such a comparison is thus probably valid only in the forward hemisphere of the emitted particle. The kinematical differences and the ϵ_f dependence can be taken into account, and one obtains

$$\frac{d^2\sigma(\mathrm{He}^3,pp)}{d\epsilon_fd\Omega_k}=\left(\frac{(m_N{}^3\epsilon_f)^{1/2}}{4\pi^2}\right)\left(\frac{2}{3}\right)$$

$$\times\left|\frac{\int\phi_{\mathrm{He}}(\xi,\mathbf{r})\chi_q{}^{-*}(\mathbf{r})d^3\xi d^3r}{\int\phi_{\mathrm{He}}(\xi,\mathbf{r})\psi_d{}^*(\mathbf{r})d^3\xi d^3r}\right|^2\frac{d\sigma(\mathrm{He}^3,d)}{d\Omega}, \tag{42}$$

where the factor in the first parentheses on the right side of Eq. (42) is the ratio of the density of available final states for the (He^3,pp) reaction to that for the (He^3,d) reaction, and the factor in the second parentheses is the corresponding ratio for the spin-isospin sums.

At low or medium energies conditions (2) and (3) cannot be met. Despite this shortcoming, it is possible to relate the cross section for the (He^3,pp) reaction to that for the (He^3,d) process by an optical-model "extrapolation", if condition (1) is valid. If, in addition, condition (4) holds, then the nuclear part of the optical potential for the pp center-of-mass interaction with the final nucleus is identical to that of a deuteron of the same energy. However, even if there is a spin- and isospin-dependent part of the optical potential, the difference between the deuteron and pp potentials can be taken into account if the dependence is known. Since this is not the case, we have neglected these differences in our work. However, we have relaxed conditions (2) and (3) and have taken into account the Coulomb and energetic differences between the pp center of mass and the deuterons produced in a (He^3,d) reaction by means of the optical model. The nuclear potential used was of the Woods-Saxon form with volume absorption. The parameters for He^3 and for d were obtained from elastic scattering,[4,11] although small variations were made to obtain an adequate fit to the (He^3,d) measured differential cross section in the forward hemisphere. The parameters actually used are listed in Table I. With these

[10] E. M. Henley, F. Richards, and D. U. L. Yu, Phys. Letters **15**, 331 (1965).

[11] J. Testoni, S. Mayo, and P. E. Hodgson, Nucl. Phys. **50**, 479 (1964).

TABLE I. Optical-potential parameters.

Helium 3

$V=-(U+iW)\{1+\exp[(r-R)/a]\}^{-1}$
$R=r_0A^{1/3}$, $r_0=1.50$ F, $a=0.6$ F,
$U=55$ MeV, $W=60$ MeV.

Deuteron

$V=-(U+iW)\{1+\exp[(r-R)/a]\}^{-1}$
$R=r_0A^{1/3}$, $r_0=1.50$ F, $a=0.6$ F,
$U=56.9$ MeV, $W=12.0$ MeV

Proton

$$V=-U\{1+\exp[(r-R)/a]\}^{-1}-iW\exp\left\{-\left(\frac{r-R}{b}\right)^2\right\}$$

$R=r_0A^{1/3}$, $r_0=1.25$ F, $a=0.6$ F, $b=0.98$ F
$U=(58-0.3E_{\text{inc}})$MeV, $W=3E_{\text{inc}}^{1/2}$ MeV
E_{inc}=Incident energy of proton

parameters, the differential cross section for the (He^3,d) reaction, given by

$$\frac{d\sigma(\text{He}^3,d)}{d\Omega}=\frac{\mu_i\mu_f}{4\pi^2}\frac{P_f}{P_i}\frac{1}{2}\frac{1}{2l+1}\frac{2J_f+1}{2J_i+1}\left(\frac{A+1}{A}\right)^2 \times B^2(t_it_f;J,J_iJ_f)(t_i\tfrac{1}{2}\nu_i\tfrac{1}{2}|t_f\nu_f)^2|d'|^2\sigma(\Theta), \quad (43)$$

with

$$d'=\frac{8\pi V_0\gamma^3 3^{3/4}}{(\beta^2+\gamma^2)^{3/2}}\int_0^\infty \psi_d^*(r) \times\exp\left\{-\frac{\beta^2\gamma^2+0.75\gamma^4}{\beta^2+\gamma^2}r^2\right\}r^2dr, \quad (44)$$

and $\psi_d(r)$=space part of the deuteron internal wave function, is compared with experiment in Fig. 2.[12] The choice of C^{12} as target was determined by (1) the availability of experimental data, and (2) the fact that it is a light nucleus for which the assumptions (a)–(e) of Sec. II are expected to be valid. The comparison made in Fig. 2 shows that good agreement can be obtained in the forward hemisphere; it should be noted that this is so for the magnitude as well as for the angular distribution. The lack of agreement in the backward hemisphere is ascribed, at least in part, to our neglect of spin-orbit effects.

All of the above description refers to the **R**, **r** formulation. In the $\mathbf{r}_1$, $\mathbf{r}_2$ formulation, the optical potential in the initial state is identical to that of the **R**, **r** formulation. The optical-potential parameters for the interaction of the protons with C^{13} were determined from elastic-scattering data, as given by Hodgson.[13]

In the calculation of the $\mathbf{r}_1$, $\mathbf{r}_2$ cross sections, there is

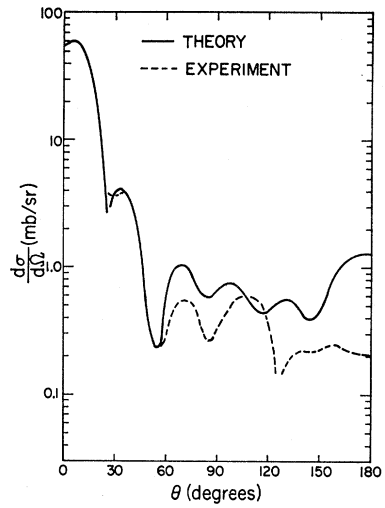

FIG. 2. Comparison between theory and experiment for the C^{12}(He^3,d)N^{13} differential cross section. The laboratory energy of the incident He^3 particle is 25 MeV.

an ambiguity regarding the momenta $\mathbf{k}_1$ and $\mathbf{k}_2$ to be used in calculating χ_1^- and χ_2^-. This is because MSCAT-4, which calculates these wave functions, assumes there is just one particle impinging on the target in the incident channel. Several schemes which might plausibly be suggested were tested by simulating plane waves for χ_K^+, χ_1^-, and χ_2^-; this is achieved by putting in zero for all optical potentials, as well as for the Coulomb interaction, in MSCAT-4. The results of this simulated plane-wave Born approximation were compared with the results of the actual plane-wave Born approximation (PWBA) [see Eqs. (49) and (50) and Fig. 9]. Best results were obtained by putting in the actual value of $\mathbf{k}_1$ and $\mathbf{k}_2$ wherever they appear explicitly in Eq. (38), but calculating χ_1^- from the relative momentum $\boldsymbol{\kappa}_1$ given by

$$\boldsymbol{\kappa}_1=\frac{\mathbf{K}'+(A+1)\mathbf{k}_1}{A+2},$$

where $\mathbf{K}'$ is the recoil momentum of the residual nucleus; the analogous procedure was employed for calculating χ_2^-.

IV. RESULTS

The differential cross section for the C^{12}(He^3,pp)C^{13} reaction was calculated with the formalism described in Sec. II and with the optical-potential parameters (except for Coulomb energy changes) discussed in Sec. III. The results for 25 MeV incident He^3 particles in the **R**, **r** formulation are presented in Figs. 3 and 5. In Fig. 3 the differential cross section is shown as a function of the pp center-of-mass angle for $\epsilon_f=1$ MeV. The choice of target and incident energy was determined by available C^{12}(He^3,d)N^{13} data; although the use of the optical model allows extrapolations to other energies, a "direct"

[12] H. E. Wegner and W. S. Hall, Phys. Rev. **119**, 1654 (1960).
[13] P. E. Hodgson, in *Direct Interactions and Nuclear Reaction Mechanisms* (Gordon and Breach, Science Publishers, Inc., New York, 1962), p. 103.

comparison [see Eq. (42)] can only be made at this energy, and is shown in Fig. 4. In Fig. 5 the ϵ_f dependence is plotted for a pp center-of-mass angle of 0°. The choice of $\epsilon_f=1$ MeV in Fig. 3 was determined by its closeness to the peak of the final-state pp interaction effect.[10] The enhancement in the cross section due to the pp rescattering can be described by the factor $F(\epsilon_f)$:

$$F(\epsilon_f)=\frac{\text{Cross section with final-state interaction included}}{\text{Cross section with final-state interaction neglected}}. \tag{45a}$$

This factor is independent of the scattering angle θ_k and depends only on the ratio

$$F(\epsilon_f)=\left|\int_0^\infty \chi_q^{-*}(\mathbf{r})\exp\left\{-\frac{\beta^2\gamma^2+0.75\gamma^4}{\beta^2+\gamma^2}r^2\right\}r^2dr\Big/\right.$$
$$\left.\int_0^\infty e^{i\mathbf{q}\cdot\mathbf{r}}\exp\left\{-\frac{\beta^2\gamma^2+0.75\gamma^4}{\beta^2+\gamma^2}r^2\right\}r^2dr\right|^2. \tag{45b}$$

This equation also demonstrates that only the S-wave part of $\chi_q^-(\mathbf{r})$ is relevant; all other angular momenta do not contribute because of the form we have chosen for the He^3 internal wave function. The dependence of $F(\epsilon_f)$ on ϵ_f is shown in Fig. 6. Comparison of this figure with Fig. 5 demonstrates that the primary ϵ_f dependence of the differential cross section in the **R**, **r** formulation arises from the final-state factor. The matrix element is a slowly varying function of the energy transfer. This slowness is also partially responsible for the similarity of the (He^3,d) and (He^3,pp) angular distributions, as can be noted from a comparison of Figs. 2 and 3.

The **R**, **r** and the $\mathbf{r}_1$, $\mathbf{r}_2$ formulations differ only through the manner in which the final-state effects are approximated. From Eqs. (6) and (23) we see that if we take the final-state distorting potentials $V(\mathbf{R}')$, $v(\mathbf{r})$, $V(\mathbf{r}_1)$, and $V(\mathbf{r}_2)$ equal to zero, then the two formulations are identical. Inclusion of the potential $v(\mathbf{r})$ introduces the final-state factor $F'(\mathbf{q})=F'(|\mathbf{q}|)=F(\epsilon_f)$. We can introduce analogous factors for the effects of the other final-state optical potentials; thus, if $G(\mathbf{k})$ is that due to $V(\mathbf{R}')$, then the cross section in the **R**, **r** formulation is $|F(\epsilon_f)G(\mathbf{k})|^2$ times that for plane waves in the final state. In the $\mathbf{r}_1$, $\mathbf{r}_2$ formulation we have factors $f_1(\mathbf{k}_1)$ and $f_2(\mathbf{k}_2)$ which arise from $V(\mathbf{r}_1)$ and $V(\mathbf{r}_2)$. [This does not imply that the factors $G(\mathbf{k})$, $f_1(\mathbf{k}_1)$, and $f_2(\mathbf{k}_2)$ are independent of the incident momentum **K**.] We note that these two interactions are equivalent to the inclusion of $V(\mathbf{R}')$ and the omission of $v(\mathbf{r})$ [or $F(\epsilon_f)$] in the **R**,**r** formulation, for $|\mathbf{R}'|\gg|\mathbf{r}|$. Since the major contribution to $F(\epsilon_f)$ comes from $r\sim R_{\mathrm{He}}\sim\gamma^{-1}$ [see Eq. (45)] and that to $G(\mathbf{k})$ arises from $\mathbf{R}'\gtrsim R_{C^{12}}$, the above condition is satisfied approximately. If this argument is realistic, then in order to compare the results of the $\mathbf{r}_1$, $\mathbf{r}_2$, and **R**, **r** formulations we should neglect $v(\mathbf{r})$ [i.e., set $F(\epsilon_f)=1$ in the **R**, **r** formulation], and should find

$$\frac{G(\mathbf{k})}{f_1(\mathbf{k}_1)f_2(\mathbf{k}_2)}\approx 1. \tag{46}$$

This relation implies that the differential cross sections in the $\mathbf{r}_1$, $\mathbf{r}_2$, and **R**, **r** formulations are approximately

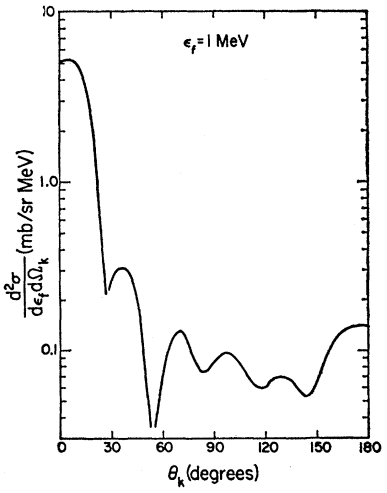

FIG. 3. Differential cross section for the $C^{12}(He^3,pp)C^{13}$ reaction in the R, r formulation, for $\epsilon_f=1$ MeV. The laboratory energy of the incident He^3 particle is 25 MeV.

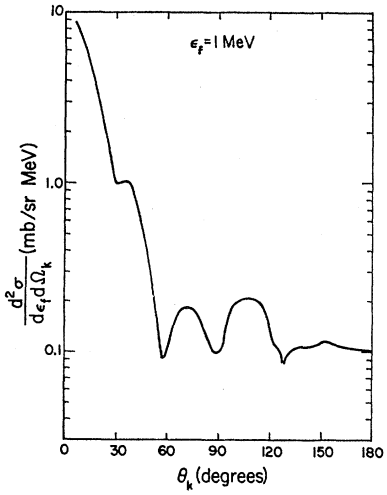

FIG. 4. Differential cross section for the $C^{12}(He^3,pp)C^{13}$ reaction predicted by a "direct" comparison with the $C^{12}(He^3,d)N^{13}$ reaction.

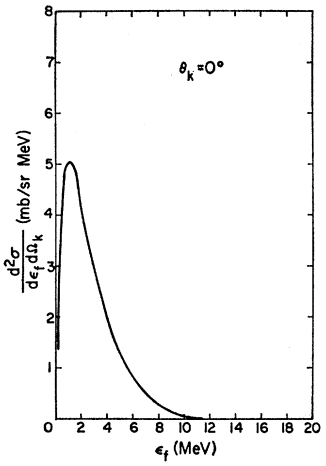

FIG. 5. Dependence on ϵ_f of the $C^{12}(He^3,pp)C^{13}$ reaction in the **R**, **r** formulation for $\theta_k=0°$. The laboratory energy of the incident He^3 particle is 25 MeV.

related by

$$\frac{d^2\sigma(\mathbf{R},\mathbf{r})}{d\epsilon_f d\Omega_k} \approx \frac{4\pi F(\epsilon_f)}{H} \frac{d^3\sigma(\mathbf{r}_1,\mathbf{r}_2)}{dE_1 d\Omega_1 d\Omega_2}, \tag{47}$$

where H is the final-state ratio given by

$$H=\frac{d\epsilon_f d\Omega_k d\omega_q}{dE_1 d\Omega_1 d\Omega_2}. \tag{48}$$

In Eq. (48) the variable ω_q refers to the angular variables for the relative momentum **q**.

The factor H depends on ϵ_f, E_1, and the angle θ_{12} between $\mathbf{k}_1$ and $\mathbf{k}_2$ (see Fig. 8). We have taken $\epsilon_f=1$ MeV as in the **R**, **r** calculation. In the $\mathbf{r}_1$, $\mathbf{r}_2$ calculation the reference point for E_1 is chosen so that $E_1=E_2$ at $\theta_1=\theta_2=0°$. The θ_{12} dependence of H gives rise to an increase of $\sim 13\%$ as θ_{12} goes from 0° to 90°, or, stated

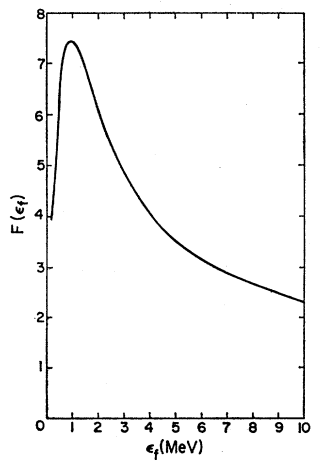

FIG. 6. "Enhancement" factor $F(\epsilon_f)$.

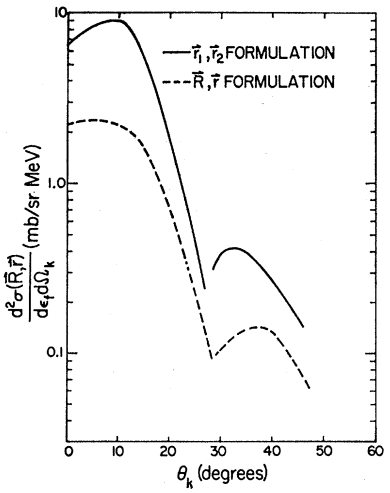

FIG. 7. Comparison of the differential cross section for the $C^{12}(He^3,pp)C^{13}$ reaction in the $\mathbf{r}_1$, $\mathbf{r}_2$ formulation, with that for the **R**, **r** formulation.

more precisely, keeping θ_1 fixed at 0° and letting θ_2 go from 0° to 90° as described below.

In order to make the comparison suggested by Eq. (47) we must have comparable physical situations. In the **R**, **r** formulation the scattering angle θ_k refers to the polar angle for **k**, the momentum of the pp center of mass. In the $\mathbf{r}_1$, $\mathbf{r}_2$ calculation we fix $\mathbf{k}_1$ at $\theta_1=0°$, its magnitude being determined by the reference point E_1 as described above, and vary the direction θ_2 of $\mathbf{k}_2$ from 0° to 90°. Under these conditions $\mathbf{k}_2$ (and hence **k**) is determined by energy-momentum conservation. As θ_2 goes from 0° to 90° the magnitude of $\mathbf{k}_2$ increases by $\sim 7\%$, introducing an error of $\sim 14\%$ due to the $1/k_2^2$ factor in the cross section. However, the 13% error introduced by neglecting the θ_{12} dependence of H is in the opposite direction, so that the over-all error is only a few percent. We have therefore simplified the $\mathbf{r}_1$, $\mathbf{r}_2$ calculation by neglecting the θ_{12} dependence of H and by taking $|\mathbf{k}_1|=|\mathbf{k}_2|=\text{constant}=2m_N E_1$. Taking $\theta_1=0°$ and $|\mathbf{k}_1|=|\mathbf{k}_2|$ implies $\theta_k=\frac{1}{2}\theta_2$.

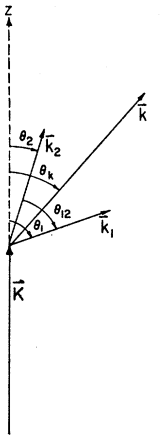

FIG. 8. Relation between the incident momentum **K** of the He^3 particle, the momentum **k** of the center of mass of the pp pair, the momentum $\mathbf{k}_1$ of proton 1, and the momentum $\mathbf{k}_2$ of proton 2.

The results of the $\mathbf{r}_1$, $\mathbf{r}_2$ formulation, calculated from the right side of Eq. (47) under the conditions just described, are shown in Fig. 7. The results from the **R**, **r** calculation are included in Fig. 7 for comparison. Both curves are normalized absolutely and have not been multiplied by any arbitrary constants. The $\mathbf{r}_1$, $\mathbf{r}_2$ calculation was carried out for only ten angles because of the large amount of computer time required for evaluating the $\mathbf{r}_1$, $\mathbf{r}_2$ matrix element.

V. DISCUSSION

The two formulations that have been used in this paper to approximate the description of the (He^3,pp) reaction are complementary ones. In the **R**, **r** formulation the interaction between the two protons is properly taken into account, and the interactions of the two protons with the daughter nucleus are approximated by one with the pp center of mass. This formulation is thus one which approximates the two-proton system by a "virtual bound-like" state. In the $\mathbf{r}_1$, $\mathbf{r}_2$ formulation the interactions of the two protons with the nucleus are replaced by optical potentials (which can be thought to approximately include the force of one proton on the other) but the interaction between the protons is not included specifically. Despite this difference, Fig. 7 shows that the angular distribution of the center of mass of the two protons is essentially the same for the two formulations. Although the magnitudes of the differential cross sections differ by a factor of approximately 3, this difference is not sufficiently large to constitute an experimentally determinable distinction, since both Eqs. (22) and (24) contain parameters which are not fully determined experimentally. Thus, as might have been expected, the angular distribution of the recoiling nucleus is primarily determined by the angular and linear momentum transfers.

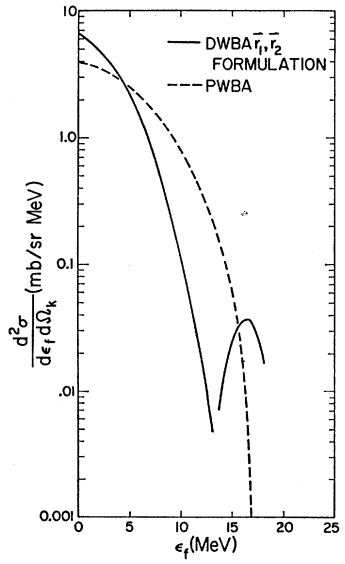

FIG. 9. Dependence of the $C^{12}(He^3,pp)C^{13}$ reaction on ϵ_f for **q** perpendicular to **k**, $\theta_k=0°$, and incident He^3 energy of 25 MeV. The PWBA result is included for comparison but is arbitrarily normalized, whereas the $\mathbf{r}_1$, $\mathbf{r}_2$ DWBA result is absolutely normalized according to Eq. (47).

The distinguishing feature of the two complementary descriptions is the treatment of the relative motion of the two protons. This suggests that measurements of their correlation could serve as a distinguishing tool. We therefore consider the dependence of the magnitude of the cross section at a fixed recoil angle as a function of the relative momentum of the two protons, **q**. We have already seen that in the **R**, **r** formulation the cross section depends only on ϵ_f or equivalently only on the magnitude of **q**, but not its direction. This dependence was shown in Fig. 5.

In the $\mathbf{r}_1$, $\mathbf{r}_2$ formulation we therefore investigate the **q** dependence of the cross section for two cases. In the first of these we keep $|\mathbf{k}_1|=|\mathbf{k}_2|=$ constant as described in Sec. IV, and vary **q** by changing the angle θ_{12} between $\mathbf{k}_1$ and $\mathbf{k}_2$ so that the direction of the pp center-of-mass momentum (i.e., **k**) is kept fixed at 0°. We see that for this situation **q** is perpendicular to **k**. The results of the $\mathbf{r}_1$, $\mathbf{r}_2$ calculation for this situation are shown in Fig. 9.

To gain some insight into the behavior of the $\mathbf{r}_1$, $\mathbf{r}_2$ cross section in Fig. 9, we turn to the plane-wave Born approximation. Inserting plane waves in the $\mathbf{r}_1$, $\mathbf{r}_2$ matrix element [Eq. (26)] we find that, under the condition that **q** is perpendicular to **k** (see Fig. 8), the PWBA overlap integral I_0 is given by

$$I_0=\text{constant}\times\int j_1(QR)\Re_1(R)\left\{\exp\left(-\frac{m_N\epsilon_f+K^2/36}{4\gamma^2}\right)+\exp\left(\frac{2m_n(V_n-E_n)}{16\gamma^2}\right)\right\}R^2dR, \quad (49)$$

where **K** is the momentum of the incident He^3, $\mathbf{Q}=\mathbf{K}-(\mathbf{k}_1+\mathbf{k}_2)$ is the momentum transfer, V_n is the potential seen by the captured nucleon, and E_n is the energy of the captured nucleon. The momentum transfer **Q** is related to the final relative energy ϵ_f by

$$\mathbf{Q}=\mathbf{K}-2\frac{A}{A+1}\left(\frac{A+1}{A+3}m_N(E-\epsilon_f)\right)^{1/2}\hat{K}, \quad (50)$$

where E is the center-of-mass energy of the entire system in the final state. The PWBA cross section (arbitrarily normalized) is included in Fig. 9; it passes through the first zero at $\epsilon_f\sim17.2$ MeV. The comparison of the DWBA and PWBA shows that the effect of the optical potentials on the ϵ_f dependence of the $\mathbf{r}_1$, $\mathbf{r}_2$ formulation is primarily to decrease the energy ϵ_f at which the first zero occurs.

For the second case **q** was varied by keeping $\mathbf{k}_1$ and $\mathbf{k}_2$ fixed in the forward direction while changing their magnitudes, so that **q** is parallel to **k**. The results of the (DWBA) $\mathbf{r}_1$, $\mathbf{r}_2$ calculation for this situation are shown

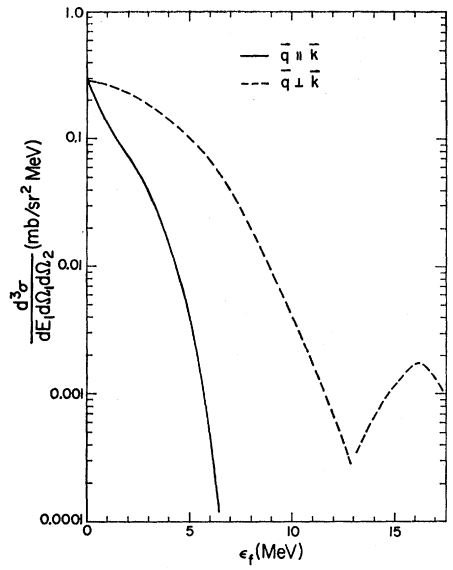

FIG. 10. Dependence of the $C^{12}(He^3,pp)C^{13}$ reaction on ϵ_f for $\mathbf{q}$ parallel to $\mathbf{k}$, $\theta_k=0°$, and incident He^3 energy of 25 MeV. The analogous result for $\mathbf{q}$ perpendicular to $\mathbf{k}$ (see Fig. 9) is included for comparison. In Fig. 10 both curves are absolutely normalized according to Eq. (40).

in Fig. 10, with the curve from Fig. 9 included for comparison. (Figure 10 exhibits the cross section $d^3\sigma/dE_1 d\Omega_1 d\Omega_2$, rather than $d^2\sigma/d\epsilon_f d\Omega_k$ [as computed from Eq. (47)] which is shown in Figs. 7 and 9.) It is clear that the latter decreases much more slowly with increasing ϵ_f. Thus, as might be expected, the cross section in the $\mathbf{r}_1$, $\mathbf{r}_2$ formulation depends on the direction of $\mathbf{q}$, as well as on its magnitude. This difference from the $\mathbf{R}$, $\mathbf{r}$ formulation serves as an experimentally distinguishable feature.

Although the comparison of the two formulations for similar conditions is of interest, it is not expected that they are applicable in the same region of phase space. For small values of the relative energy ϵ_f, the $\mathbf{r}_1$, $\mathbf{r}_2$ formulation is expected to be a poor approximation, and the $\mathbf{R}$, $\mathbf{r}$ formulation is clearly preferred. The reason is that the two protons are closely correlated in the incident He^3, and they will therefore continue to interact strongly with each other if the two protons in the final state emerge in the same general direction with approximately equal energies. In fact, as can be seen from Fig. 9, the cross section in the $\mathbf{r}_1$, $\mathbf{r}_2$ formulation fails to go to zero as ϵ_f approaches zero; that it should vanish in this limit is due to the Coulomb repulsion between the two protons, which has been neglected.

For large relative energy ϵ_f, on the other hand, we expect the $\mathbf{R}$, $\mathbf{r}$ formulation to be poor. In this case, the two protons emerge in quite different directions, so their final-state rescattering would be expected to be small. In other words, for large ϵ_f, the "enhancement factor" $F(\epsilon_f)\approx 1$, and we expect the interaction of the two protons with the final nucleus to be more important than that of the two protons with each other, which is strong only in a relative S state of angular momentum.

Thus, we see that there are two extremes, namely small ϵ_f, where the $\mathbf{R}$, $\mathbf{r}$ formulation is expected to be reasonable, and large ϵ_f, where the $\mathbf{r}_1$, $\mathbf{r}_2$ formulation is preferable. In the intermediate region the extrapolation of the two complementary pictures can serve as a guide. However, it is quite possible that a more complicated Faddeev-type four-body treatment is required; this could even be true in the limiting situations of small and large ϵ_f. Within the context of our development, the most crucial difference between the various formulations appears to be measurements of the correlations between the two protons.

In the above discussion we have concentrated on the reaction mechanisms for the (He^3,pp) reaction. However, as stated earlier there is another aspect of this process which is of interest. It can be used, in conjunction with (d,p) reactions, for spectroscopic studies. In both cases a neutron is captured by the initial nucleus; however, differences can occur due to core excitation, e.g., change of isospin of $\frac{3}{2}$ in the (He^3,pp) reaction, as well as due to the differences of the internal structure of deuteron and He^3. A further interest of the reaction is thus to explore these differences, if they exist.

VI. ACKNOWLEDGMENTS

The authors wish to thank I. Halpern for helpful comments and suggestions. They also thank D. U. L. Yu for the use of the computer code to calculate $\sigma(\Theta)$, and the University of Washington Computer Center for free computer time.